THE JOURNAL OF PHYSICAL CHEMISTRY B

ARTICLE

pubs.acs.org/JPCB

Hydrogen Evolution from Formic Acid in an Ionic Liquid Solvent: A Mechanistic Study by ab Initio Molecular Dynamics

B. L. Bhargava,[†,‡,§] Yoshiro Yasaka,[†,§] and Michael L. Klein[*,†]

[†]Institute for Computational Molecular Science, Temple University, 1900 N. 12th Street, Philadelphia, Pennsylvania 19122, United States

[‡]Laboratory for Research on the Structure of Matter, University of Pennsylvania, 3231 Walnut Street, Philadelphia, Pennsylvania 19104-6202, United States

Supporting Information

ABSTRACT: The reversible decomposition of formic acid ($HCOOH \rightleftharpoons CO_2 + H_2$) has been attracting attention for its potential utility in hydrogen storage and production. It is therefore of interest to explore the influence of solvents on the decomposition reaction. To this end, Born−Oppenheimer (BO) molecular dynamics (MD) calculations have been performed to explore the mechanism involved in hydrogen (H_2) evolution from formic acid decomposition in an ionic liquid solvent. Specifically, for a solvent consisting of 1,3-dimethylimidazolium cations and formate anions, evolution of hydrogen (H_2) and carbon dioxide (CO_2) was observed within a few picoseconds when BO-MD trajectories were carried out at an elevated temperature of 3000 K. The observed dehydrogenation involved a reaction between a formic acid solute and a nearby solvent formate anion. The observed mechanism contrasts with the unimolecular mechanism proposed in the gas phase. Specifically, in the ionic liquid, the reaction is initiated from a C−H bond dissociation of a formate anion to produce a short-lived hydride anion, which subsequently captures the acidic proton of a nearby formic acid molecule. The present BO-MD computations suggest that the high reducing ability of formic acid in the ionic liquid is due in part to its acid-dissociated form: the formate anion, which is encouraged to dissociate into a hydride anion and CO_2 by the strong electrostatic field of the ionic liquid solvent.

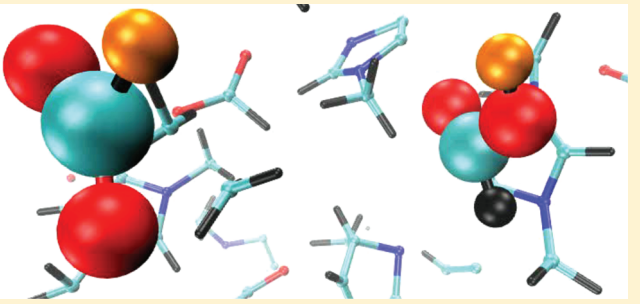

INTRODUCTION

Hydrogen is the ultimate clean fuel, whose use could solve a number of environmental issues caused by combustion of fossil fuels. However, one drawback of hydrogen fuel arises from the low liquefaction temperature since fuel compactness and fluidity, as attained in the liquid state, are typically necessary for the low-cost transportation and storage. Recently, formic acid has been gaining increasing attention as a compact hydrogen energy source.[1,2] Formic acid is one of the oldest known and most well-studied organic molecules, but even so a number of new aspects in its chemistry and physics have emerged recently.[3−5] The underlying strategy of using formic acid as a hydrogen energy source is encapsulated by the following reversible reactions:[6]

$$HCOOH \rightleftharpoons CO + H_2O$$

$$HCOOH \rightleftharpoons CO_2 + H_2$$

The first equation enables formic acid synthesis from CO, which can be easily derived from various waste or biological carbon sources. The more important step is the second reaction, which allows both hydrogen storage and production. Controlling the direction and the rate of the latter reaction are essential for application. Thus, a number of studies have been carried out seeking efficient and environmentally favorable ways to accomplish this end.[7,8]

The interesting properties and potential for industrial applications of room temperature ionic liquids (ILs) are becoming increasingly widely recognized.[9] ILs are nearly vapor free and recyclable solvents that can facilitate a number of organic reactions.[10] The unique solvation of reactants by ions in ILs is known to play a significant role in the reaction kinetics and equilibrium. There is growing interest on ways to control the selectivity, rates, and yields of the competing decompositions. Recently, experimental evidence was reported on the large solvation effect of ILs on the equilibrium constant of formic acid decarboxylation.[8] Importantly, this experimental work failed to

Special Issue: H. Eugene Stanley Festschrift

Received: April 29, 2011
Revised: June 17, 2011
Published: July 20, 2011

uncover the mechanism of the hydrogen evolution from formic acid that occurred in the absence of a metal catalyst. Accordingly, in the present computational study, we have attempted to unravel the relevant reaction mechanism.

Ab initio molecular dynamics (AIMD) can provide valuable insights into mechanisms of chemical reactions in condensed phases.[11] Direct dynamical simulations have the advantage that they require neither a priori knowledge on reaction coordinates nor the actual chemical forms (acid-dissociated, protonated, coordinated, etc.) of reactants and products. This contrasts with the situation prevailing for traditional energy barrier calculations employing known or intuitively reasonable reaction coordinates. Direct application of AIMD allows one to probe a number of possible chemical reaction pathways involved in a given system. Indeed, AIMD has already been applied to get insights into hydrogen-bond reorganization and acid dissociation.[12,13] However, many chemical reactions involving breakage of more stable chemical bonds are very slow, typically orders of magnitude slower than the periods of molecular vibrations and rotations. Due to this huge gap in time scale, direct AIMD is often augmented with powerful sampling methods.[14−16]

Given that a reaction probability is typically governed by its activation energy, reactions are expected to occur at an exponentially increasing rate by raising the system temperature. Of course, raising the temperature does not necessarily accelerate the motion of molecules along the needed reactive trajectory. Nevertheless, it can be expected that unknown reaction mechanisms operating in the experimental conditions can also occur and thus be discovered in temperature-accelerated simulations. Although novel sampling methods are available to probe rare events (e.g., metadynamics[14]), they generally require some a priori knowledge or intuitive guess concerning the key reaction coordinates. Thus, they are difficult to adapt to explore as yet unknown reactions and their associated mechanisms. Instead, they can play a useful role in further elaboration of any newly unveiled mechanism. Temperature-accelerated AIMD was recently applied to study hydrogen (H_2) production from borane compounds.[17] In the present exploratory survey study, we have probed the formic acid dehydrogenation mechanism by applying BO-MD as implemented in the CPMD code.[18] Anticipating our results we will see that a BO-MD trajectory carried out at a temperature of 3000K yields a short-lived hydride anion as an intermediate in the evolution of hydrogen from formic acid in an ionic liquid.

METHODS

Born−Oppenheimer molecular dynamics (BO-MD) simulations of formic acid in the IL (see Figure 1), 1,3-dimethylimidazolium formate ([mmim][HCOO]) were performed at 3000 K using the CPMD code.[18] All hydrogen atoms were assumed to be deuterated. Nevertheless, we simply use the symbol "H" rather than "D" in chemical formula below. The system studied consisted of 12 ion pairs plus 6 neutral formic acid molecules. In total, the simulated system consisted of 270 atoms and 780 valence electrons. The ions and molecules were initially dispersed randomly within a cubic box of edge length 16.24 Å. Three-dimensional periodic boundary conditions consistent with cubic box were employed to simulate bulk behavior. The initial configuration for the BO-MD simulations was obtained from a 1.5 ns classical MD simulation performed at 1000 K and atmospheric pressure using standard force fields.[19,20] Norm

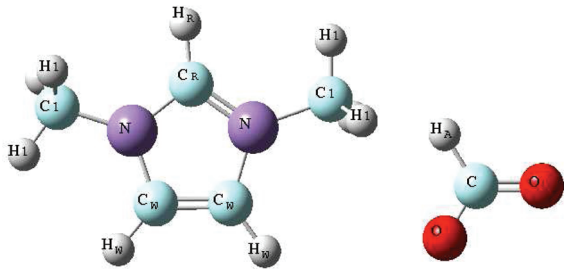

Figure 1. Molecular structure and nomenclature of the ionic liquid 1,3-dimethylimidazolium formate ([mmim][HCOO]).

conserving pseudopotentials of the Troullier−Martins form[21] were used to consider the interaction between the nuclei and core electrons. The cutoff radii of the pseudopotentials were as follows; 0.500 (S orbital) and 0.3838 (P orbital) for deuterium; 1.23(S), 1.23 (P), and 0.7159 (D) for carbon; 1.12(S), 1.12 (P), and 0.6031 (D) for nitrogen; 1.12(S), 1.12 (P), and 1.12 (D) for oxygen. Gradient corrected exchange and correlation functional prescribed by Becke[22] and Lee et al.[23] were employed. The electronic orbitals were expanded in a plane wave basis set with an energy cutoff of 90 Ry. The kinetic energy of the ions was controlled using Nosé-Hoover chain thermostats.[24] A time step of 10 au (0.24 fs) was used to integrate the equations of motion over a trajectory spanning 3 ps. Positions and velocities of each nucleus was stored every time step and were subsequently used for the analysis. At each step, optimally localized valence-electron Wannier centers were computed from appropriate Wannier functions.[25] Another system with a single ion pair and a single formic acid molecule was simulated within a cubic box of 12 Å at 3000 K (denoted as single ion-pair simulation). Starting from different initial positions and velocities, 5 independent reactive trajectories were obtained. Other details for this simulation were identical to that of previously mentioned system.

RESULTS AND DISCUSSION

The simulation system initially contained 12 formate anions and 6 formic acid molecules. During the 3-ps BO-MD run, we observed three types of reactions: (a) hydrogen evolution events involving formate anions and formic acid, (b) fast proton transfer between formic acid molecules and formate anions, and (c) fragmentation involving 10 out of the 12 imidazolium cations that decomposed by the end of the run. Importantly, the competitive decomposition of formate anion/formic acid and the imidazolium cation has been already observed experimentally.[26] It is likely that the high temperature employed in the simulation has accelerated these reactions.

As already mentioned, we observed the formation of a hydrogen molecule (H_2) from the reactants formic acid plus the formate anion during the course of the simulation. The reaction mechanism is illustrated in Figure 2 by snapshots taken from a reactive trajectory. The reaction was initiated by the vibrational excitation of the formate anion C−H bond (see: snapshots Top and Center).

$$HCOO^- \rightarrow H^- + CO_2$$

As the C−H bond becomes elongated, the H atom dissociated, leaving behind carbon dioxide. Importantly, the Wannier dipole analysis showed that the hydrogen was accompanied with

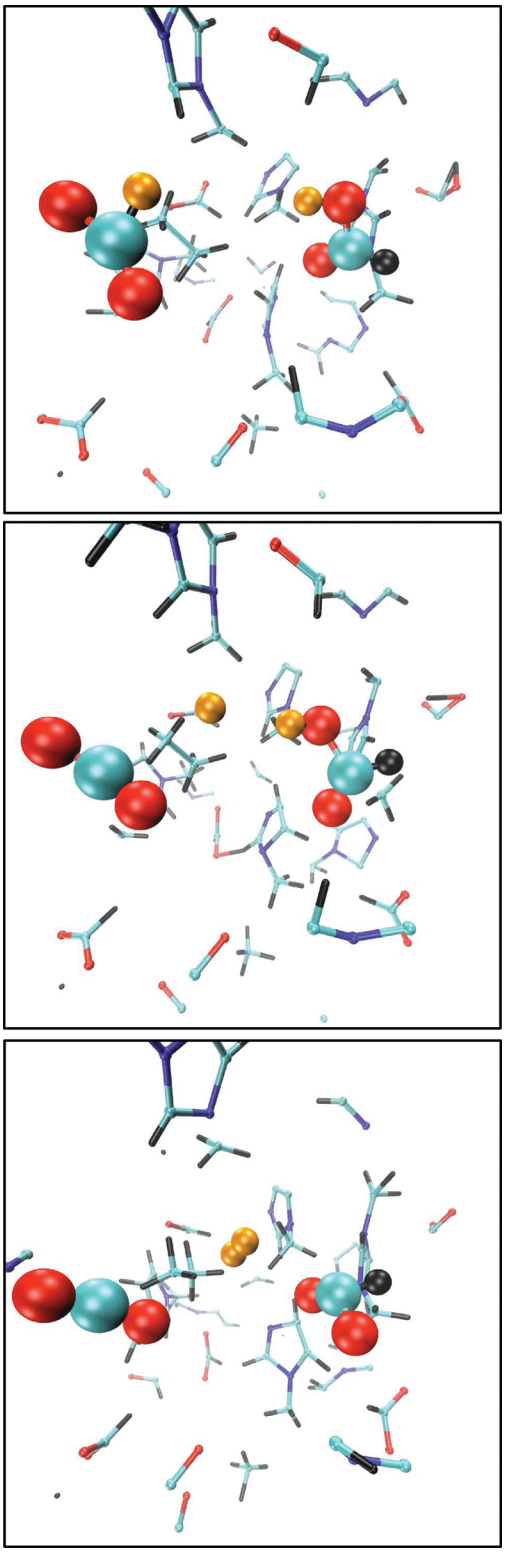

Figure 2. Snapshots of a part of the system containing formic acid in an ionic liquid showing the hydride anion intermediate and subsequent H_2 formation. (Top) The two molecules involved in the formation of H_2 are drawn with enlarged ball and stick representation: red (oxygen); cyan (carbon); black (passive hydrogen); gold (active hydrogen). (Center) The hydride anion has dissociated from the formate anion and is between the CO_2 and HCOOH molecules. (Bottom) The hydride anion captures the acidic proton of HCOOH to form H_2.

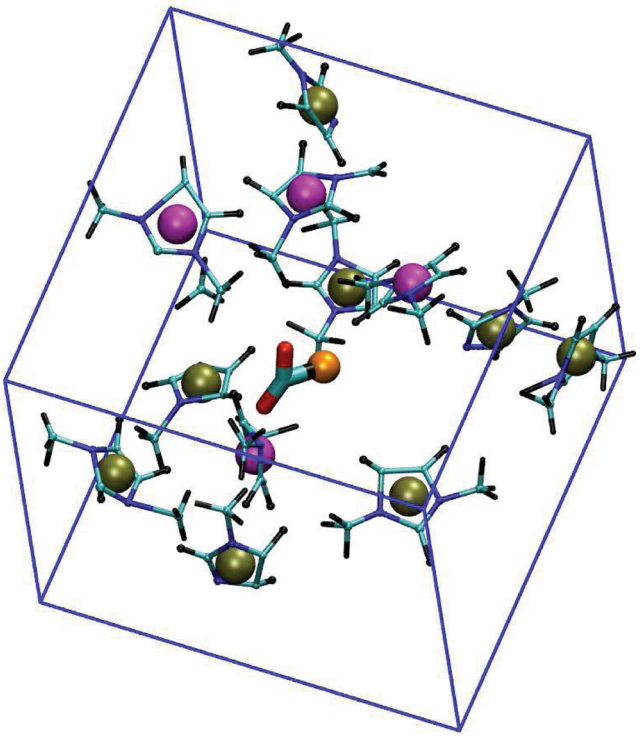

Figure 3. Cation distribution around the hydride (orange sphere) dissociating from formate anion just before the dissociation. The ring centers of the cations within 8 Å of the hydride anion are shown by magenta spheres and those farther than 8 Å by brown spheres, respectively.

an electron pair. Thus, the hydrogen atom released from the formate anion is actually a short-lived hydride anion. In the Center snapshot, the hydride intermediate is ~3 Å away from the C atom of CO_2 and approaching an acidic proton of a nearby HCOOH molecule. Only 50 fs after the C−H bond breakage, the hydride anion coupled with the acid proton, leaving a formate anion (snapshots Center to Bottom).

$$H^- + HCOOH \rightarrow H_2 + HCOO^-$$

Since the first (hydride dissociation) and the second (hydride-proton recombination) steps did not occur simultaneously but consecutively, the dehydrogenation reaction can be regarded as a two-step reaction (although not perfectly separated) rather than a single-step reaction. The first step should have a much higher barrier than the second. Thus, the observed reaction mechanism predicts molecular hydrogen formation to be rate-limited by the initial hydride dissociation, an event that should be accessible to ultra fast spectroscopic experiments.

The coordination structure of the cation (ring center) around the hydride anion immediately before its dissociation from the formate anion is shown in Figure 3. The hydride anion was coordinated by 4 cations within 8 Å and 11 cations within 10 Å. The closest cation was found at a distance of ~5 Å. This suggests that the hydride intermediate is stabilized in the strong charge-ordered structure of the IL solvent. As in other AIMD studies,[27] the structure of the IL is characterized by strong charge ordering. The calculated radial distribution function (RDF) shows that in [mmim][HCOO] formate is surrounded by, on average, 6 cations belonging to the first solvation shell. The first peak was

observed at 5.2 Å (see Figure S1). This solvation structure stabilizes the formate anion in the IL. When the hydride anion dissociates from the formate, it moves to the nearby anion solvent shell, which is a good potential well for any anion. Thus, the local electrostatic field readily stabilizes the hydride anion whenever it is formed. The lifetime of the hydride anion is, however, very short because of its intrinsic high chemical reactivity.

The H_2 formation mechanism observed here is different from the one previously proposed for the gas phase. The gas-phase decomposition of formic acid into hydrogen and CO_2 is considered to be a unimolecular reaction.[28] In this mechanism, the cis conformation (two hydrogen atoms on the same side of the C−O axis) of formic acid facilitates H_2 elimination. The cis formic acid is also considered as the actual reactant in hydrothermal conditions.[29] In the present study, in contrast, H_2 formation involved two molecules: a formate anion and a formic acid molecule. In the latter mechanism, the reactivity of the formate anion plays the key role. Clearly, the formate anion is not important in formic acid decomposition carried out in the gas-phase or under hydrothermal conditions (unless base is added), and thus its role in formation of H_2 has been paid less attention. The two reaction mechanisms can be distinguished by a kinetic study. In the unimolecular mechanism, the kinetics should be first order in the concentration of formic acid added to the solvent. Thus, the H_2 formation rate should depend linearly on the concentration of formic acid in the IL. In contrast, the hydride-mediated kinetics should be first order in the formate anion concentration. As the formate anion is the solvent in this case, the reaction rate should be (nearly) constant irrespective of the concentration of formic acid added to the solvent.

A similar reaction pathway for the formation of H_2 was observed in 2 of the 5 single ion-pair BO-MD simulations. The difference from the liquid simulation mentioned above was that the short-lived hydride anion traveled a larger distance to couple with the acidic proton of the formic acid molecule.

In the larger BO-MD simulation, we could sample another reactive trajectory involving the short-lived hydride-anion. In this reaction, the hydride anion released from a formate anion coupled with a proton of CH_3^+ to form methane. The reactant CH_3^+ was dissociated earlier from an imidazolium cation. A similar reaction producing methane was observed in 2 of 5 single ion-pair BO-MD simulations, but this time the hydride anion attacked the methyl carbon of the intact imidazolium cation and performed a nucleophilic substitution reaction, with the leaving group being methylimidazole. The latter result suggests that a short-lived hydride anion can react in many ways other than coupling with the acidic proton in formic acid. This is expected because the hydride anion is so reactive that it can attack any nearby positive charge to form more or less stable chemical bonds.

Two other reactions involving formic acid and formate anion were observed in the larger BO-MD simulation. One of the two was unimolecular dehydration (equivalently, decarbonylation) of HCOOH to form CO and H_2O. The mechanism observed was the same as proposed in the gas phase studies. The C−O bond of formic acid broke to produce HCO^+ and OH^-, immediately followed by a proton migration from HCO^+ to OH^-. The second reaction was initiated from the C−H bond breakage of a formate anion, but in this case the dissociated hydrogen atom was positively charged, leaving CO_2 with an electron pair. The electron pair then jumped to a fragment of a decomposed

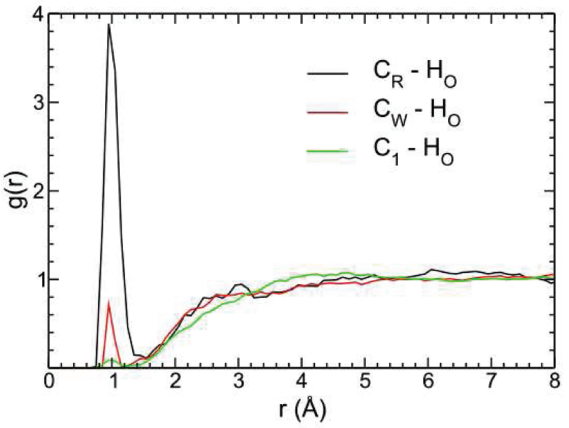

Figure 4. Radial distribution functions, $g(r)$, for the hydroxyl proton (H_O) of formic acid around three atomic sites on the imidazolium cation. The nomenclature of the cation atomic sites is shown in Figure 1.

imidazolium cation. We consider that some of the reaction pathways, including this one, observed under extreme temperature and pressure conditions are not likely to be important in experiments carried out at or near ambient conditions.

The chemical inertness of an IL is a major concern when it is considered as reaction medium. Organic cations constituting ILs, such as imidazolium and quaternary ammonium cations, are known to be not very stable, because of the polarized chemical bonds (C−H, N−C) near the charge center. In our BO-MD simulations, the imidazolium cation was not stable. Out of 12 cations, only 2 were intact after 3 ps. One of the cations fragmented into two parts with the destruction of the aromatic ring. The remaining cations turned into charge-neutral methyl imidazole or unsubstituted imidazole by losing methyl group(s) on the N atom. According to experimental studies, the imidazolium cation is not stable and tends to lose a methyl group by the attack of bases and nucleophiles.[30] The formate anion is a relatively strong base, and thus methyl-group elimination is likely to occur.

In addition to the chemical reactions discussed above, a number of proton transfers were observed. The proton sites involved in proton transfers can be identified by examination of appropriate RDFs. When a proton H_X attached to a heavy atom X is exchanged with H_Y attached to Y, the RDF for H_X−Y and H_Y−X will show an intramolecular peak. RDFs of acidic proton (H_O) of formic acid around the carbons (C_R, C_W, and C_1) of the imidazolium cation (shown in Figure 4) suggest the proton transfer probability from the formic acid to the cation. The amplitude of the intramolecular peak is in the order of $C_R > C_W > C_1$ pair. This is consistent with the known acidity of the protons: $H_R > H_W > H_1$. Thus, even at 3000 K, BO-MD is able to reasonably reproduce the acidity of protons in O−H and C−H bonds. This fact strengthens the reliability of our approach of elucidating mechanisms of chemical reactions from high-temperature BO-MD.

We also calculated the RDFs between the CH hydrogen (H_A) of formic acid (or formate anion) and the imidazolium carbons (C_R, C_W, and C_1). In all cases, the intramolecular peaks were negligibly small, which implies C−H bonds tend to dissociate as $C^+\cdots H^-$ rather than $C^-\cdots H^+$. The exceptional case where the C−H hydrogen turned into a proton was when HCOOH decarbonylated to form H_2O.

CONCLUSIONS

By employing direct BO-MD calculations at an elevated temperature (3000 K) we have been able to elucidate the reaction mechanism of formic acid decomposition in an ionic liquid. We appear to have discovered a new mechanism of hydrogen (H_2) evolution involving the formate anion. The formate anion first dissociates into a hydride anion and CO_2 and the former then abstracts an acidic proton from a nearby formic acid molecule. In ILs, the hydride anion intermediate is significantly stabilized by the local electrostatic field arising from the charge-ordered IL structure, which thus plays a key role in facilitating H_2 formation. Based on the present simulation results, we expect the following to be verified experimentally to confirm the hydride-mediated H_2 formation mechanism. First, the decarboxylation rate is nearly independent of formic acid concentration because the rate-limiting step is the dissociation of the C−H bond of the formate anion. Second, there are expected byproduct such as methane when the intermediate hydride reacts with the imidazolium cation. Consequently, more CO_2 is produced than H_2. A corollary of our findings is that in order to prevent the formation of unwanted byproduct, the cation of the IL should be inert against hydride anion attack. Here, the imidazolium ion is not a good choice, because the imidazole ring protons are relatively acidic and the carbons next to the nitrogen atoms have an electrophilic character. Possibly phosphonium-based ILs will show higher stability and thus can give a higher yield of H_2. In future work we plan to elaborate on the mechanism of the hydride-mediated hydrogen evolution in the IL by more sophisticated sampling methods such as metadynamics. In addition, we plan to employ a QM/MM approach to expand the system size as well as investigating the role of dispersion interactions.

ASSOCIATED CONTENT

Supporting Information. Radial distribution functions for the solvent cations and anions (Figure S1) and a movie showing H_2 evolution. This material is available free of charge via the Internet at http://pubs.acs.org.

AUTHOR INFORMATION

Corresponding Author

*Phone: +1-215-204-1927. Fax: +1-215-204-2257. E-mail: bhargav@sas.upenn.edu (B.L.B.); yoshiro.yasaka@temple.edu (Y.Y); mlklein@temple.edu (M.L.K.).

Author Contributions

§Contributed equally to the work.

ACKNOWLEDGMENT

We are grateful to Masaru Nakahara for many stimulating discussions and continuing interest in this work. The research was supported in part by RAK-CAM through the award of a Sheikh Saqr bin Mohammad al Qasimi Research Fellowship.

REFERENCES

(1) Enthaler, S.; von Langermann, J.; Schmidt, T. *Energy Environ. Sci.* **2010**, *3*, 1207–1217.

(2) Fukuzumi, S.; Kobayashi, T.; Suenobu, T. *ChemSusChem.* **2008**, *1*, 827–834.

(3) Minary, P.; Jedlovszky, P.; Mezei, M.; Turi, L. *J. Phys. Chem. B* **2000**, *104*, 8287–8294.

(4) Chelli, R.; Righini, R.; Califano, S. *J. Phys. Chem. B* **2005**, *109*, 17006–17013.

(5) Bako, I.; Hutter, J.; Palinkas, G. *J. Phys. Chem. A* **2006**, *110*, 2188–2194.

(6) Kroschwitz, J. I.; *Encyclopedia of chemical technology*, 4th ed.; Wiley: New York, 1991.

(7) Yasaka, Y.; Yoshida, K.; Wakai, C.; Matubayasi, N; Nakahara, M. *J. Phys. Chem. A* **2006**, *110*, 11082–11090.

(8) Yasaka, Y.; Wakai, C.; Matubayasi, N; Nakahara, M. *J. Phys. Chem. A* **2010**, *114*, 3510–3515.

(9) Kirchner, B. *Top. Curr. Chem.* **2009**, *290*, 213–262.

(10) (a) Welton, T. *Chem. Rev.* **1999**, *99*, 2071–2083. (b) *Ionic liquid in synthesis II*; Wasserscheid, P., Welton, T., Eds.; Wiley-VCH: Weinheim, Germany, 2007.

(11) Geissler, P. L.; Dellago, C.; Chandler, D.; Hutter, J.; Parrinello, M. *Science* **2001**, *291*, 2121–2124.

(12) Wang, S.; Bianco, R.; Hynes, J. T. *J. Phys. Chem. A* **2009**, *113*, 1295–1307.

(13) Dopieralski, P. D.; Latajka, Z.; Olovsson, I. *Acta Crystallogr.* **2010**, *B66*, 222–228.

(14) Laio, A.; Parrinello, M. *Proc. Natl. Acad. Sci. U.S.A.* **2002**, *99*, 12562–12566.

(15) Bolhuis, P. G.; Chandler, D.; Dellago, C.; Geissler, P. L. *Annu. Rev. Phys. Chem.* **2002**, *53*, 291–318.

(16) Bonomi, M.; Parrinello, M. *Phys. Rev. Lett.* **2010**, *104*, 190601.

(17) Li, J.; Kathmann, S. M.; Hu, H.; Schenter, G. K.; Autrey, T.; Gutowski, M. *Inorg. Chem.* **2010**, *49*, 7710–7720.

(18) CPMD version 3.13.2, http://www.cpmd.org/, Copyright IBM Corp. 1990−2008, Copyright MPI fuer Festkoerperforschung, Stuttgart, 1997−2001.

(19) (a) Vanommeslaeghe, K.; et al. *J. Comput. Chem.* **2010**, *41*, 671. (b) Force field parameters for formic acid and formate were adapted from those for formamide and acetic acid shown in the parameter file available at http://mackerell.umaryland.edu/CHARMM_ff_params.html > toppar_c35b2_c36a2.tar.gz > par_all22_prot.inp; (c) Atomic charges used are as follows: H_{CHbond}(−0.03), C(0.75), $O_{carbonyl}$(−0.55), $O_{hydroxyl}$(−0.61), and $H_{hydroxyl}$(0.44) for formic acid; H(−0.10), C(0.62), and O(−0.76) for formate.

(20) (a) Lopes, J. N. C.; Deschamps, J.; Padua, A. A. H. *J. Phys. Chem. B* **2004**, *108*, 2038. (b) Lopes, J. N. C.; Deschamps, J.; Padua, A. A. H. *J. Phys. Chem. B* **2004**, *108*, 11250.

(21) Troullier, N.; Martins, J. L. *Phys. Rev. B* **1991**, *43*, 1993–2006.

(22) Becke, A. D. *Phys. Rev. A* **1988**, *38*, 3098–3100.

(23) Lee, C.; Yang, W.; Parr, R. G. *Phys. Rev. B* **1988**, *37*, 785–789.

(24) Martyna, G. J.; Klein, M. L.; Tuckerman, M. E. *J. Chem. Phys.* **1992**, *97*, 2635–2643.

(25) Marzari, N.; Vanderbilt, D. *Phys. Rev. B* **1997**, *56*, 12847–12865.

(26) Nakahara, M.; Matubayasi, N.; Yasaka, Y. Japan Patent in press.

(27) Zahn, S.; Thar, J.; Kirchner, B. J. *Chem. Phys.* **2010**, *132*, 124506.

(28) Blake, P. G.; Hinshelwood, C. *Proc. R. Soc. London, Ser. A* **1960**, *255*, 444.

(29) Yagasaki, T.; Saito, S.; Ohmine, I. *J. Chem. Phys.* **2002**, *117*, 7631–7639.

(30) Glenn, A. G.; Jones, P. B. *Tetrahedron Lett.* **2004**, *45*, 6967.